Received: 12 October 2022 | Revised: 13 January 2023 | Accepted: 18 January 2023 | Published on: 9 February 2023

DOI: 10.1002/ctpp.202200161

ORIGINAL ARTICLE

Contributions to Plasma Physics

Simulation of the statistical and formative time delay of Townsend-mechanism-governed breakdown in argon at low pressure

Aleksandar P. Jovanović[1] | Marjan N. Stankov[1] | Vidosav Lj. Marković[2] | Suzana N. Stamenković[2]

[1]Leibniz Institute for Plasma Science and Technology (INP), Greifswald, Germany

[2]Department of Physics, Faculty of Sciences and Mathematics, University of Niš, Niš, Serbia

Correspondence
Aleksandar P. Jovanović, Leibniz Institute for Plasma Science and Technology (INP), Felix Hausdorf Str. 2, 17489 Greifswald, Germany.
Email: aleksandar.jovanovic@inp-greifswald.de

Funding information
Deutsche Forschungsgemeinschaft, Grant/Award Numbers: 407462159, 466331904; Ministarstvo Prosvete, Nauke i Tehnološkog Razvoja, Grant/Award Number: 451-03-68/2022-14/200124

Abstract

Understanding the breakdown process is important both from fundamental and practical perspectives. One of the most important quantities that characterize the breakdown is the breakdown time delay. In this article, numerical models for self-consistent simulation of the statistical and formative time delay of the electric breakdown in argon at low pressure have been proposed. The first model, based on the Monte Carlo simulation of the electron avalanche development, is used to simulate the statistical time delay. The model is designed for low-pressure breakdowns when the Townsend mechanism is dominant. The electric breakdown is then governed by ion-induced secondary electron emission from the cathode. In that case, the statistical time delay to breakdown is determined by tracking the waiting time of emission of the primary electron that initiates the electron avalanche and the number of ions produced in it. On the other hand, the formative time delay is determined by simulating the electric current waveform $I(t)$ using the fluid model. To test whether the proposed models can be used for discharges operating under various conditions, the voltage dependence is simulated for both the statistical and the formative time delay. The results of the simulations show good agreement with the experimental results and theoretical models.

KEYWORDS

electron avalanches, fluid model, Monte Carlo simulation, time delay

1 | INTRODUCTION

The electric breakdown of gases is of great importance for technological applications, primarily for the operation of gas-controlled switches, voltage and current breakers, and for high voltage systems where gas is used as an insulator.[1–3] A full understanding of how various parameters influence gas breakdown is crucial for better control of the discharge and predicting its behaviour under different conditions. Most applications of electrical discharges require that the initiation (ignition) phase be tightly controlled. However, discharge is determined by many factors that cannot always be controlled by experimental conditions. Prediction of the discharge behaviour, therefore, often requires the development of

sophisticated physically-based models, providing various information about the processes of initiation and establishment of electric discharge. In this article, we propose such models for the description of breakdown time delay.

The electric breakdown of gases is not an instantaneous process, and some time between applying the voltage and the breakdown usually exists. The time between the application of the voltage greater than the static breakdown voltage and the breakdown of the gas is known as the breakdown time delay or time lag t_d.[4] It consists of two components, the statistical t_s and formative t_f time delay. Statistical time delay is the time between applying a voltage greater than the static breakdown voltage and the appearance of the initial electron that initiates the breakdown.[4] Formative time delay is the time that elapses from the occurrence of initiating electron until the collapse of applied voltage and the occurrence of a self-sustained current.[4] It is well known that the statistical and the formative time delay are stochastic variables,[5–10] and numerous statistical models were often used to describe their distributions and behaviour under various conditions.[7–13] The important aspect often lacking in these models is the possibility of predicting the time delay without additional assumptions (such as the time delay distribution). Here, we will use a different approach. By trying to model underlying physical processes that occur during the breakdown, the statistical and formative time delay will be determined.

A lot has already been done regarding the numerical modelling of electric breakdowns, but new analyses are not out of the question. Electric breakdown of gases, in general, has been widely studied in the literature.[14–24] For instance, the Monte Carlo method of electron transport has been used to determine the breakdown criterion for the low-pressure Townsend breakdown in helium and investigate electron bursts under the homogeneous electric field.[14] The radio-frequency breakdown in low-pressure argon has been studied in Reference [15], while low-pressure Townsend discharge in hydrogen has been modelled in Reference [16]. Besides low pressure, particle models have also been used for modelling an atmospheric-pressure streamer breakdown in References [17–19]. The Monte Carlo model is used to investigate streamer initiation and formation in atmospheric air in Reference [17], taking into account photoionisation in the model. The streamer initiation in atmospheric pressure gas is simulated by the two-dimensional (2D) particle model, and the interaction between the avalanches and self-induced field is studied in Reference [18]. Besides particle models, fluid modelling was used to describe the Paschen curve in different gases.[22–24] Most of these articles mainly focus on the breakdown criterion. Recently, the time delay has been considered in the state-of-the-art particle-in-cell (PIC) modelling of helium discharge,[20,21] while the time delay of the streamer discharge was investigated in Reference [19]. Three stages in the breakdown process have been identified, and the effect of the various parameters on the delay time is reported in Reference [21].

In this article, we deal with the Townsend-mechanism-governed discharge and propose two physically-based numerical models for the time delay modelling. The presented models for the breakdown time delay, although similar to other models from the literature,[19,21] have their own advantages. Namely, most of the reported models focus on the total time delay. Here, we will try to distinguish between the statistical and formative time delays and model each separately. The first model is used to simulate statistical time delay. Since the statistical time delay is determined by a single initial electron that starts the electron avalanche leading to breakdown, the particle model is most suitable for its description. Furthermore, the statistical time delay marks the early period of the discharge, when the external field is still unperturbed by space charge, so the use of this model is appropriate. Therefore, the Monte Carlo model of electron avalanche, which takes into account binary interactions of electrons with the atoms in the gap, is used to simulate the statistical time delay of breakdown, its distribution, and the voltage dependence. On the other hand, the formative time delay, as its name implies, represents the period during which the discharge fully forms. The accumulated space charge in the discharge gap and numerous processes occurring during the establishment of the discharge makes the particle model unsuitable for the description of formative time delay. The formative time delay is conversely determined from the macroscopic quantity, that is, by calculating the current waveform and its steep rise to the stationary value using the fluid model.

The structure of the paper is as follows. In Section 2, a detailed description of the models is given. The experiment set-up and procedure used to measure the data for validation of the models are briefly described in Section 3. In Section 4, the simulation results are presented and compared to the analytical model and experimental results. In the last section, a short summary is given.

2 | METHODS

2.1 | Monte Carlo modelling of discharge inception and statistical time delay

To simulate the statistical time delay, we need to determine when the "successful" electron (electron that initiates the avalanche that leads to breakdown) is emitted. For simplicity, we will discuss the case of a low preionisation level (i.e., the

low level of residual charges remained from the previous discharge) when the time between two consecutive emissions of the initial electron is large. Let us assume that the initial electron is emitted by some weak radiation from the cathode. Note that the initial electron may be produced in the gas as well, but with a much lower probability. In that case, the electron emission follows the Poisson distribution,[25] while the waiting time for electron emission t_{ee} then follows the exponential distribution. If the waiting time for electron emission is much larger than ion transit time, which is the case for a low preionisation, the moment of occurrence of a successful electron can be determined by monitoring the development of the subsequent avalanches initiated by ion-emitted secondary electrons. To do this, the particle-based model described in Reference [26] has been employed.

The spatially three-dimensional (3D) Monte Carlo model used to simulate the electron avalanches in a constant and uniform electric field is described, verified and validated elsewhere.[26] Note that the model uses the null collision method to determine the electron collision time, while the isotropic scattering of the electrons has been assumed. The model is extended to include the motion of ions as well, for which only the elastic collisions have been considered. Using this model, the number of ionisations in the gap, that is, the number of produced electrons and ions is calculated. Due to the exponential growth of the electron avalanche, most ions are produced near the anode. In the first approximation, let us assume that all ions drift with the constant drift velocity v_i towards the cathode and that all arrive without any loss. Then the ion transit time in inter-electrode space with distance d is equal to $t_i = d/v_i$. For chosen conditions, ion transit time is much smaller than the time between two consecutive emissions of the initial electron. The problem is now to determine if the initial electron was successful and whether the breakdown criterion is fulfilled. In Reference [14], the criterion of the breakdown, that is, the critical state, is defined as the voltage at which the average number of created ions in an electron avalanche is just enough to liberate at least one new electron from the cathode. Starting from this criterion, one can extend it for the determination of the successful electron.

Let us assume that every avalanche is initiated by a single electron at the cathode. The number of electrons in an avalanche in the inter-electrode space is equal to $N_e = e^{\alpha d}$, where α is Townsend's first ionization coefficient and d is inter-electrode space distance. The total number of ions produced by an avalanche initiated by an initial electron is then equal to $N_i = e^{\alpha d} - 1$. Note that at low pressure, the recombination is negligible. For Townsend's mechanism, the breakdown criterion is determined by the secondary electron emission by ions. The number of secondary electrons is determined by the boundary condition $\mathbf{\Gamma}_e = -\gamma \mathbf{\Gamma}_i$, where $\mathbf{\Gamma}_e$ and $\mathbf{\Gamma}_i$ are the fluxes of electrons and ions, respectively, while γ is the secondary electron emission coefficient. Here, we assume that the reflection of ions can be neglected. Since we are dealing with the early phase of discharge, the external field is unperturbed by a space charge, so it is safe to assume that ion velocity is constant. It follows that

$$N_e = \gamma N_i \geq 1, \tag{1}$$

which will be used as a criterion for a successful initial electron. Namely, if a single electron emitted from the surface produces enough ions to emit one or more secondary electrons in the next cycle, then this electron is treated as successful. However, even though this method is good for the determination of the critical state (voltage), that is, breakdown voltage, it cannot be applied to calculate the statistical time delay. This approach calculates the average number of ions but does not consider the development of the secondary avalanches initiated by the secondary electrons. Namely, if any subsequent secondary avalanche is unsuccessful, the next primary avalanche will be initiated by a new primary electron, with a new waiting time t_{ee}. Thus, if we do not consider the secondary avalanches, the calculated statistical time delays are much shorter than expected.

To overcome this challenge, the procedure is slightly modified. Instead of using the average number of created ions, we track every secondary avalanche and check whether the criterion for breakdown is fulfilled. If the criterion is fulfilled, the statistical time delay is equal to the sum of emission times of the initial electron until the successful outcome. Otherwise, the simulation is reset, and a new initial electron is tracked until the criterion for breakdown is fulfilled.

The described model is appropriate for the ideal case when the diameter of the electrodes is much larger than the inter-electrode distance ($D \gg d$). Then, all ions from the gap reach the cathode. On the other hand, in more realistic situations, when electrode diameter is comparable to the inter-electrode space, some ions may be lost on the tube walls. In order to describe this loss, the model is modified to include ion transport. In this case, we track every ion produced in the gap on its way to the cathode, the same way as we do for the electrons.[26] Note that the null collision method is used here as well.[27] Based on the number of ions arriving at the cathode and the breakdown criterion (1), it is determined whether the primary electron was successful. Finally, for the most accurate description, we would need to track every ion that arrives at the cathode and simulate secondary electron emission, similar to in Reference [28]. However, that would make the model quite complex and significantly prolong the calculation time.

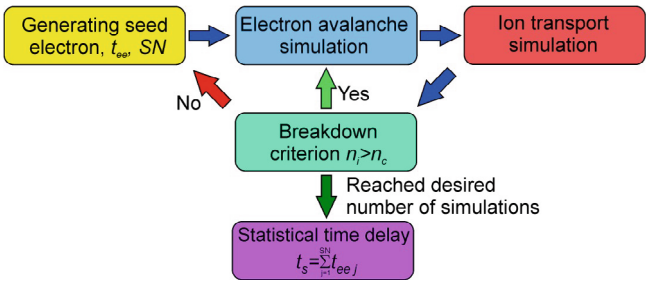

FIGURE 1 Flow chart of the statistical time delay simulation procedure with included ion transport. Here, SN denotes the seed number, that is, an ordinal number of the initial electron, while t_{ee} is the waiting time for electron emission. In a simplified approach, the ion-transport step can be skipped by assuming that all the ions have reached the cathode. In that case, the breakdown criterion is determined from the total number of produced ions in the gap.

In Figure 1, the schematic illustration of the simulation procedure is displayed. The primary electrons are emitted from the cathode at the time interval t_{ee} (following the exponential distribution), which is randomly generated. The primary electron avalanche is simulated, and the position of every ionization collision, which happens during it, is stored in the memory. These positions are used as the starting position of ions in the gap in ion transport simulation. In the next step, we simulate ion transport to determine how many ions reached the cathode. We check then if the breakdown criterion (1) is satisfied, that is, if enough secondary electrons (at least one) have been emitted to continue the cycle. If it is, we repeat the electron avalanche simulation for the avalanches initiated by the secondary electrons. If the breakdown criterion is fulfilled for the desired number of secondary avalanches, then the breakdown will occur, and the statistical time delay is equal to the sum of waiting times for the initial electron

$$t_s = \sum_{j=1}^{SN} t_{ee\,j}. \tag{2}$$

If any of them does not satisfy the breakdown criterion, we return to the first step and emit the new primary electron.

The simulations in this work are carried out in argon. The cross sections for electron collisions are obtained from Reference [29] while for Ar^+ ion collisions in argon gas, the cross sections are obtained from Reference [30] database.

The whole simulation is repeated a predefined number of times to obtain the set of statistical time delay data. Due to the long computational time, we simulated between 100 and 500 data in one set. For high voltages, avalanches are large, so the calculation time is long. On the other hand, for low working voltages, near breakdown voltage, it takes a long time to pass for a successful electron to appear, prolonging calculations even more. Note, that the method works successfully for the case when $t_{ee} > t_i$.

It should be noted that the proposed method is quite similar to the first two phases described in Reference [21]. The difference is that we deal just with the discharge initiation and stop our simulation when the breakdown condition is fulfilled. The model is reduced to the determination of the number of ionization events and ion transport (used to account for their loss to the tube walls). Focussing on the early phase of the discharge initiation when the space charge is not high enough to disturb the external electric field, allows us to avoid solving the Poisson's equation and trace each produced particle separately. This approach is sufficient for the determination of the statistical time delay, while for the complete time delay description, the PIC model as in Reference [21] would be required.

2.2 | Fluid modelling of the formative time delay

Although the Monte Carlo-based model could be easily extended to determine the formative time (or the total delay time, using the PIC approach as in Reference [21]), the required computational effort would be high. Therefore, here, we rely on more efficient fluid modelling. The drawback is that the fluid model is deterministic, so only a single, that is, the average value of the formative time delay can be determined. The advantage, however, is an option to use it for different levels of preionisation and its fast computational times.

Let us assume that the initial electron has appeared very quickly after applying the voltage and that the statistical time delay is negligible. In that case, the formative time delay is the time between the application of voltage and the occurrence of a self-sustained current. By using the simple fluid model, from the calculated voltage and glow current waveforms ($U(t)$ and $I(t)$) (see further results and discussion) the formative time delay is determined as an interval between voltage application and current rise to 90 per cent of its stationary value.

The fluid models of different complexity can be used to describe the discharge at low pressure. In our previous works, the time-dependent one-dimensional (1D) simple and extended fluid models have been successfully used to model the breakdown voltage and Paschen curve, the current–voltage characteristics, and the current and voltage waveforms.[23,24] Here, we utilize the simple fluid model[24] to determine the formative time. A brief overview of the fluid model is given as follows.

The simple fluid model comprises a set of continuity equations for electrons and ions

$$\frac{\partial n_e}{\partial t} + \nabla \cdot \mathbf{\Gamma}_e = S_e \tag{3}$$

$$\frac{\partial n_i}{\partial t} + \nabla \cdot \mathbf{\Gamma}_i = S_i \tag{4}$$

where n_e is electron number density, n_i is the number density of ions, $\mathbf{\Gamma}_e$ is electron flux, $\mathbf{\Gamma}_i$ is ion flux, while S_e and S_i are the source terms of electrons and argon ions, respectively. Electric potential and field ($\mathbf{E} = -\nabla(\phi)$) are calculated using the Poisson equation:

$$\nabla \cdot (-\nabla\phi) = \frac{\rho}{\varepsilon_0}, \tag{5}$$

where ρ is space charge density, while ε_0 is vacuum permittivity. The external circuit is included in the model using Ohm's law:

$$U_g = U_w - I_g R \tag{6}$$

where U_g is the glow voltage, U_w is the working voltage, I_g is the glow current, and R is resistance. Glow current is calculated from the total flux of charged particles at the anode as:

$$I_g = \sum_{p=1}^{N} q_p \Gamma_p S \tag{7}$$

where q_p is the charge of particle species p, N denotes the number of charged species and S is the surface area of the electrode. Since the fast-rising step voltage has been used in the experiment and the modelling, that is, after the initial fast increase, there is no change in the voltage, and the displacement current can be considered negligible on the long-time scale.

The drift-diffusion approximation is used for the particle fluxes. Since we are mainly interested in an early phase of the discharge, that is, the moment the breakdown occurs, the local field approximation (LFA) has been used. The modelling is carried out in argon. The model considers three particle species, electrons, ground-state argon atoms Ar, and atomic Ar^+ argon ions. Since we are dealing with low-pressure modelling and do not consider the relaxation processes, Ar_2^+ ions are omitted from the model. The set of partial differential equations is solved using the finite difference method, using the Scharfetter-Gummel approximation.[31] More details about the fluid model, the numerical procedure, the reaction scheme, and the used coefficients can be found in Reference [32].

3 | EXPERIMENTAL DETAILS

In order to validate the models, the simulation results have been compared to the experimental data measured in argon at low pressure. Since the measurements have been done over a long period, different tubes have been used for measurements. Namely, the experiment is carried out on two discharge tubes filled with argon (with less than 1 ppm of impurities)

at pressures 133.3 Pa (tube 1) and 226.6 Pa (tube 2), respectively, and a vacuum chamber with variable pressure and gap distance. Both tubes and vacuum chamber are of cylindrical shape and made of borosilicate glass (Schott technical glass 8245). The electrodes are plane-parallel, with an electrode diameter of 2.2 cm, approximately equal to the inner tube diameter. In the case of the vacuum chamber, the electrodes are plane-parallel with a diameter of 2.8 cm, with a glass tube of approximately the same inner diameter placed around the electrodes. This way, the electrodes are tightly fitted inside the gas tube to prevent long path breakdowns. The first tube has electrodes made of oxygen-free high-conductivity (OFHC) copper, set 0.9 cm apart. The cathode in the second tube is made of OFHC copper, while the anode is made of stainless steel (AISI 304). This tube has a variable inter-electrode distance. For this particular set of measurements, it was fixed to 1 cm. In the vacuum chamber, both electrodes are made of OFHC copper and, for this set of measurements, the distance was fixed at 1 cm.

The total time delay was determined using the electronic system for time delay measurements described in Reference [8]. The statistical and formative time delays are determined from the statistical analysis of the total time delay data. More about the measuring procedure can be found in References [8,33].

4 | RESULTS AND DISCUSSION

4.1 | Statistical time delay modelling in argon at low pressure

To test the proposed model for statistical time delay and determine its prediction accuracy, the comparison of simulation results to the analytic model and the experiment has been performed. The measurements are carried out in a vacuum chamber filled with argon at 133.3 Pa, with an inter-electrode distance of 1 cm and relaxation time $\tau = 1\,\mathrm{s}$, conditions chosen to be within the validity of the model. The same discharge parameters have been used as input in the model.

Figure 2 exhibits the comparison of the statistical time delay distribution obtained from the simulated (symbols) and measured (bars) data for the applied voltage $U_a = 400\,\mathrm{V}$. The measured data have been presented in a form of a histogram (bars in Figure 2) normalized by the bin size multiplied by the number of data. It is expected that the waiting time governed by the Poisson emission would follow the exponential distribution. To test this, the data are compared to the exponential distribution fit (solid red line)

$$f(t_s) = \frac{1}{\bar{t}_s} e^{-\frac{t_s}{\bar{t}_s}} \tag{8}$$

where $\bar{t}_s = 3.78 \times 10^{-4}\,\mathrm{s}$ is the mean statistical time delay. A good agreement between the model and the experiment can be observed. The simulation results closely follow the measurements and analytic expression, confirming that good

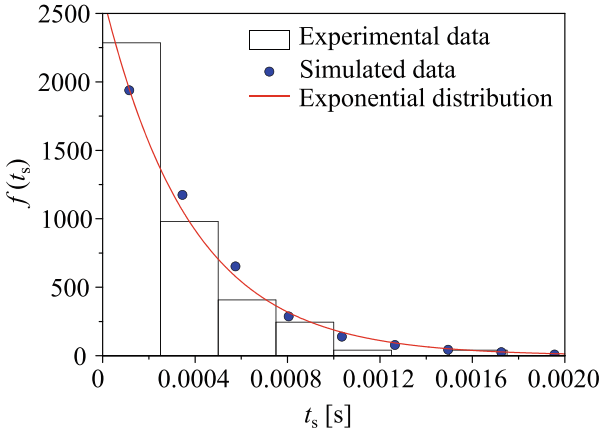

FIGURE 2 Probability density function of the statistical time delay measured in argon at pressure $p = 133.3$ Pa, with inter-electrode distance $d = 1$ cm at working voltage $U_w = 400\,\mathrm{V}$. The measured data are presented as a histogram, blue symbols represent the probability density function of the simulation results (500 data in a set), and a solid line is an exponential distribution fit of the measured data. Note that the histogram has been normalized by the bin size multiplied by the number of data.

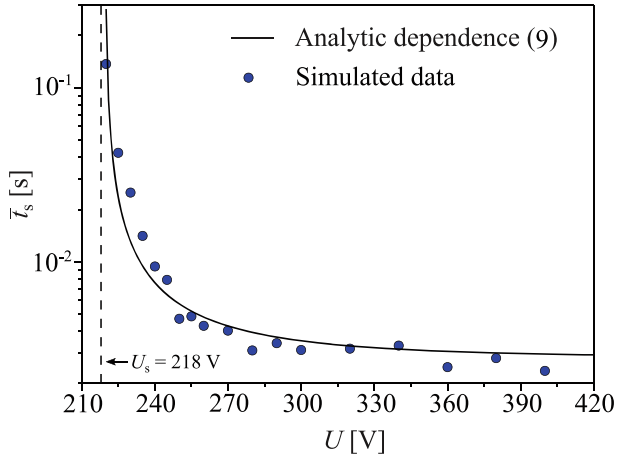

FIGURE 3 The mean statistical time delay as a function of the applied voltage. The comparison of the theoretical model (8) and the simulated mean statistical time delay for pressure $p = 133.3$ Pa, inter-electrode distance $d = 1$ cm, and relaxation time $\tau = 1$ s. Electron yield for this relaxation time is $Y = 1/2.791 \times 10^{-3}\,1/\text{s}$.

prediction can be obtained for the given conditions. Note that for considered high voltage, the probability for ionization is high, resulting in a large number of produced ions. This leads to the earlier fulfilment of the breakdown condition, usually within the first couple of initial electrons. From this, it is confirmed that the distribution of the statistical time delay is fully determined by the distribution of the electron emission waiting time, which is the exponential distribution.

To further test the proposed numerical model, the voltage dependence of the statistical time delay has been simulated and compared to the analytic model and measured data.

In Figure 3, the comparison of the simulation results and the analytic model for the voltage dependence of the mean statistical time delay $\bar{t}_s(U)$ is displayed. The voltage dependence is obtained from the breakdown probability[4,34] as

$$\bar{t}_s(U) = \frac{1}{YP} = \frac{1}{Y\left(1 - \frac{1}{\gamma(U)\left(e^{\alpha(U)d}-1\right)}\right)} \tag{9}$$

where Y represents the electron yield, γ is the secondary electron emission coefficient, α is the Townsend ionization coefficient, and d is the inter-electrode distance. The analytic model considers voltage dependence of the secondary electron emission using field dependence from Reference [35]. The field-dependent Townsend ionization coefficient is also taken from Reference [35]. Electron yield for this relaxation time is $Y = 1/2.791 \times 10^{-3}\,1/\text{s}$ (determined for the conditions of high (over)voltage where the breakdown probability is $P \approx 1$[36]). The simulation results are obtained by averaging the set of 500 statistical time delay data obtained from the numerical model. Note that slight oscillation in the data occurs due to limited dataset size. Increasing the sample would, however, significantly prolong the calculation times, especially near the breakdown voltage.

A good agreement between the analytic dependence and the simulation results can be observed in Figure 3. The numerical model closely follows the analytic dependence, describing the decrease and saturation of the statistical time delay for higher voltages and its steep increase near the breakdown voltage properly. For high voltages, ionization probability is so high that the secondary electron emission no longer influences the breakdown condition, which is fulfilled for the first emitted electron. For lower voltages, the avalanche size decreases; thus, the secondary electron emission becomes influential. The breakdown does not occur with the first emitted electron, and the statistical time delay increases. As the applied voltage decreases, the avalanches cannot provide a high enough number of ions to continue the charge carrier production immediately, so the waiting time is prolonged. For the voltages near the breakdown voltage, the condition is rarely fulfilled, and the statistical time delay tends to infinity.

The situation complicates when additional ion losses exist in the discharge chamber. To illustrate the influence of the finite dimensions of the discharge chamber, the electron avalanche initiated by an initial electron emitted from the centre of the cathode and the spatial distribution of ions arriving at the cathode surface, for two values of the applied voltage, is presented in Figure 4. The initial electron starts an avalanche by ionizing neutral atoms on its way to the anode.

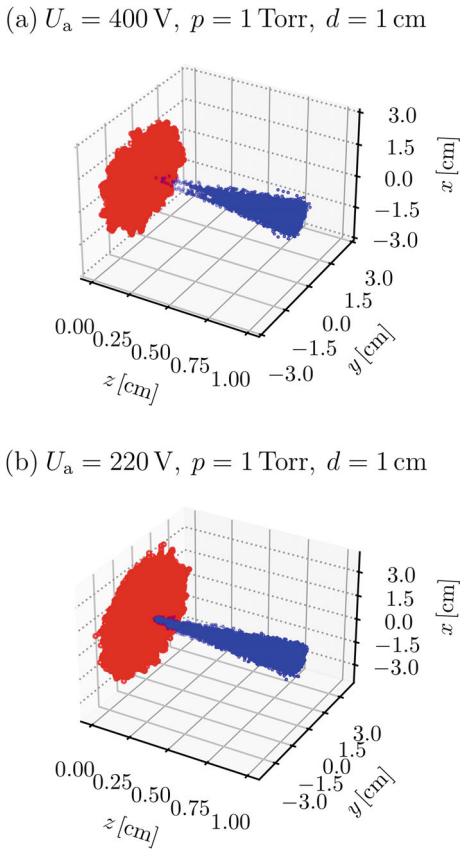

FIGURE 4 The primary electron avalanche, illustrated by produced electron-ion pairs (blue symbols) and the spatial distribution of ions after their arrival at the cathode surface (red symbols), for applied voltage $U_a = 400\,\mathrm{V}$ (a) and $U_a = 220\,\mathrm{V}$ (b).

Each position of the ionizing event represents the position of a newly produced electron-ion pair. The newly produced electrons continue to ionize neutrals until they reach the anode. The produced ions, on the other hand, drift from their starting position towards the cathode at $z = 0$. Due to their scattering in collisions with neutral atoms, the characteristic spatial distribution of ions can be seen on the cathode surface at the moment of their arrival. For a higher voltage, the electron avalanche and consequently ion distribution on the cathode become more narrow (radius of 1.5 cm in Figure 4a) in comparison to the lower voltage (radius of 3 cm in Figure 4b).

The analytic model (9) does not consider any loss processes. However, as the voltage decreases, the radial loss becomes stronger (see Figure 4b) and may highly influence the time delay. That means that the analytic model needs to be corrected for the case when the inter-electrode space is much larger than the radial dimensions of the discharge chamber. This problem becomes more pronounced if the location of each ion is taken as the starting point for the emission of the secondary electrons required to continue the charge-production loop. For this particular case considered here, for lower voltages, the radial ion loss would be significant if the radius of the discharge chamber is lower than 1.5 cm. Therefore, to overcome this challenge, ion transport needs to be considered.

As a final test of the proposed model, the direct comparison of the simulated and measured voltage-dependent mean statistical time delay is presented in Figure 5. The experiment was performed at a pressure of $p = 133.3$ Pa, an inter-electrode distance of $d = 1$ cm, and a relaxation time $\tau = 1$ s on a tube with the electrode and the tube diameter of $D = 2.8$ cm. The same parameters have been used as input in the model. At the chosen relaxation time, the preionisation is low, so it may be assumed that "seed" electron emission follows the Poisson distribution. As previously shown, since the diameter of the electrodes is not much larger than the inter-electrode distance, the radial ion loss to the tube walls had to be included in the model to properly describe the voltage dependence of the statistical time delay. Namely, it is assumed that the ion is lost if it reaches the wall, that is, if its radial position at the moment of the arrival is larger than the electrode radius. From the comparison of the results, an excellent agreement between experimental and simulated data has been achieved. The model closely follows the measured data for wide ranges of applied voltage.

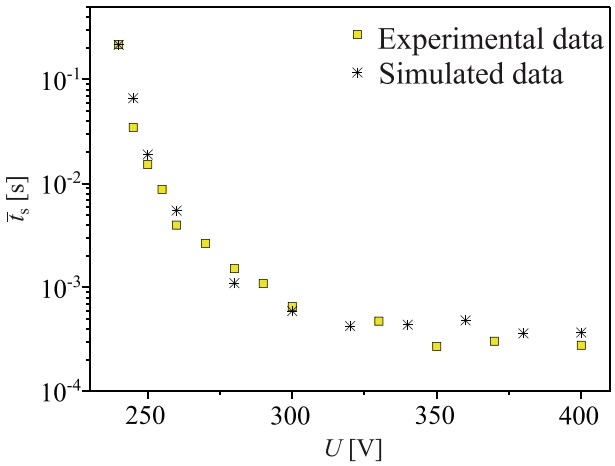

FIGURE 5 The mean statistical time delay as a function of applied voltage. The pressure is $p = 133.3$ Pa, inter-electrode distance $d = 1$ cm, electrode diameter $D = 2.8$ cm, and relaxation time $\tau = 1$ s.

The presented results show that the model successfully describes statistical time delay for various values of applied voltage just by using already available cross sections, electron yield, and field-dependent secondary electron emission coefficient as an input. Unlike vast statistical models, no further assumptions or approximations are required to describe the experiment correctly. Furthermore, the shown results confirm the importance of the avalanche statistics, that is, the number of ionization events, on the statistical time delay. More precisely, the statistical time delay is fully determined by the number of produced ions required for the fulfilment of the breakdown condition. That means that the voltage dependence influences the size of the avalanche, that is, the breakdown probability.

4.2 | Formative time delay modelling in argon at low pressure

To test the accuracy of the proposed method for the formative time determination, modelling of low-pressure glow discharge in argon has been performed. The modelling results are compared to the experimental data measured on the tubes filled out with argon at a pressure of $p = 133.3$ and 226.6 Pa, with an inter-electrode distance of $d = 0.9$ and 1 cm, respectively, for the stationary glow current of $I_g = 100$ μA. Note that the relaxation time $\tau = 1$ ms, for which the statistical time delay is negligible, has been chosen for all the measurements.

Figure 6 exhibits the comparison of the modelled and measured current waveforms. The step voltage pulse with 225 V amplitude is applied to the argon-filled tube at $t = 0$. The pressure in the tube is $p = 133.3$ Pa, while the inter-electrode distance is $d = 0.9$ cm. Using the ballast resistor ($R = 113$ $k\Omega$), the glow current has been limited to the stationary value of $I_g = 100$ μA. Note that a single current waveform is presented here, that is, averaging of the multiple experimental waveforms has not been performed. The same values of the applied voltage and the resistance were used as input in the fluid model. The formative time delay is determined as an interval between the application of the voltage and the increase of the current to 90% of its stationary value, both in the experiment and the model. A relatively good agreement between modelled and measured results can be observed. The modelled current reproduces a steep current increase quite well, although the stationary value has been reached a bit (ca. 7 μs) earlier than in experiment, that is, the model predicts a formative time of $t_f = 117.8$ μs, while the measured one is $t_f = 124.62$ μs. The reason for this discrepancy lies in the complexity of the model. Namely, the model assumes a simple circuit with only a ballast resistor. In an experiment, however, it is hard to eliminate the stray capacitance or additional parasitic resistance. Notwithstanding, considering the small influence on the results, it is reasonable to use this simplified model.

Figure 7 shows the voltage dependence of the formative time delay obtained from the experiment and the fluid modelling for two pressures, $p = 133.3$ and 226.6 Pa. In both cases, the voltage dependence of the formative time delay is measured using the variable resistor in the circuit, limiting the current to a constant stationary value of 100 μA. The short relaxation time has been chosen to assure a high preionisation level, that is, a short statistical time delay. To take into account the voltage dependence of the secondary electron emission, the model uses the field-dependent secondary

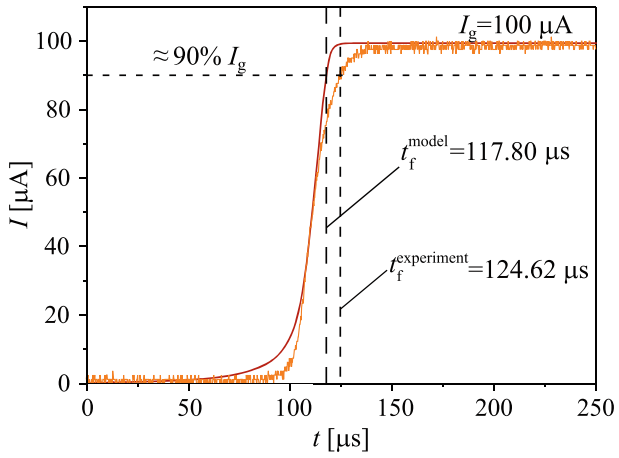

FIGURE 6 Illustration of the formative time delay determination from the current waveform $I(U)$.

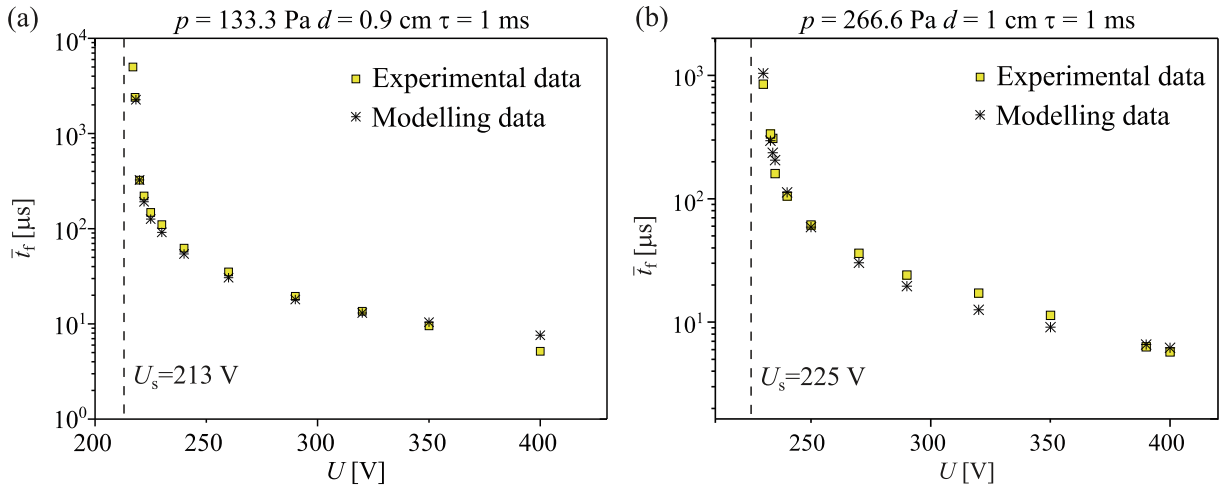

FIGURE 7 Formative time delay in argon as a function of voltage at pressure $p = 133.3$ Pa and inter-electrode distance $d = 0.9$ cm (a) and pressure $p = 226.6$ Pa and inter-electrode distance $d = 1$ cm (b). In both cases, the glow current is $I_g = 100$ μA and relaxation time is $\tau = 1$ ms.

electron emission coefficient determined from the breakdown condition. These values closely follow the value of secondary electron emission reported in Reference [35]. An excellent agreement between the modelling and measured data can be observed in Figure 7. The formative time is fully determined by the voltage dependence of the secondary electron emission coefficient, Townsend's first ionization coefficient, and ion drift velocity. The model reproduces the steep increase in the formative time delay near the breakdown voltage. On the other hand, with the increase of the applied voltage, the formative time delay shows a slightly decreasing tendency, which the model again reproduces. This tendency can be explained by increased charge carrier production and faster reaching of the stationary condition.

5 | SUMMARY

The numerical models for the description of the statistical and formative time delay to breakdown have been developed in this work. The models have been described in detail and applied to model the breakdown time delay of low-pressure argon discharge. The proposed models can completely describe the time delay in Townsend-mechanism-governed breakdowns. Furthermore, they enable one to predict the discharge behaviour under different conditions (such as pressure or applied voltage).

The modelling of the statistical time delay is performed using a particle model based on the Monte Carlo simulation of the electron avalanches. The statistical time delay is determined by the fulfilment of the breakdown condition. The model considers binary collisions of a primary electron with the gas atoms and the avalanche development. It is used to determine the number of secondary electrons produced by ions and to check when the breakdown condition is fulfilled. To properly describe the time delay in a discharge with a narrow tube, the ion transport and their loss to the walls had to be taken into account in the model as well. To validate the model, the simulations of the statistical time delay distribution and the dependence of the time delay on the applied voltage have been carried out and compared to the analytic model and experimental results. The obtained voltage dependence has been first compared to the analytical model, and good agreement has been observed. The numerical model provides insight into how different processes influence the time delay. The finite dimensions of the gas discharge tube explain the discrepancy between the numerical results and the experiment. Considering the ion losses on the discharge tube, excellent agreement with the experiment has been achieved.

Since the formative time delay is determined from the later phases of the discharge, when the number of electrons is quite large, the fluid model had to be utilized for the simulation. Namely, the formative time delay is determined by modelling the current waveform. The breakdown criterion is determined from the increase of the current to 90% of its stationary value. The voltage dependence simulation has been performed and compared to the experiment to validate the model. Again, the model and the measured data are in excellent agreement.

Although the models are self-consistent, the value of the secondary electron emission coefficient plays a significant role in the accuracy of the model prediction. For this particular case, reliable results for different values of the reduced electric field exist in the literature. However, that is not the case for other gases, so this is a significant challenge for reliable numerical modelling of the voltage-dependent time delay.

ACKNOWLEDGEMENTS

Funded by the Deutsche Forschungsgemeinschaft (DFG, German Research Foundation)—project numbers 407462159 and 466331904. V. Lj. M. and S. N. S. are grateful to the Ministry of Education, Science, and Technological Development of the Republic of Serbia for partial financial support (contract number 451-03-68/2022-14/200124). Most of the work (the core of the formative time delay model development and analysis) has been carried out as a part of M. N. S.'s PhD Thesis[33] at the University of Niš and during A. P. J.'s and M. N. S.'s work on the project ON171025 of the Ministry of Education, Science and Technological Development of the Republic of Serbia. The authors wish to thank Dr. Markus M. Becker for valuable comments and suggestions. Open Access funding enabled and organized by Projekt DEAL.

DATA AVAILABILITY STATEMENT

The data that support the findings of this study are available from the corresponding author upon reasonable request.

REFERENCES

[1] M. Kristiansen, A. H. Guenther, in Electrical Breakdown and Discharges in Gases, Part B (Eds: E. E. Kunhardt, L. H. Luessen), Plenum Press, New York **1983**, chapter Plasma Applications, p. 402.
[2] L. G. Cristophorou, S. R. Hunter, From Basic Research to Applications, in Electron-Molecule Interactions and Their Applications, Academic Press, New York **1984**.
[3] T. Shao, G. Sun, P. Yan, J. Wang, W. Yuan, Y. Sun, S. Zhang, *J. Phys. D: Appl. Phys.* **2006**, *39*(10), 2192.
[4] C. G. Morgan, in Electrical Breakdown of Gases (Eds: J. M. Meek, J. D. Craggs), John Wiley & Sons, Chichester **1978**, chapter Electrical Breakdown of Gases, p. 656.
[5] K. Zuber, *Ann. Phys.* **1925**, *76*, 231.
[6] M. von Laue, *Ann. Phys.* **1925**, *76*, 721.
[7] J. V. Kiselev, in Proc. 7th Int. Conf. Phenomena in IonizedGases (Belgrade, Yugoslavia) 838 (in Russian), **1965**.
[8] V. Lj. Marković, S. R. Gocić, S. N. Stamenković, *J. Phys. D: Appl. Phys.* **2006**, *39*(15), 3317.
[9] V. Lj Marković, S. R. Gocić, S. N. Stamenković, *J. Phys. D: Appl. Phys.* **2009**, *42*(1), 015207.
[10] V. Lj. Marković, A. P. Jovanović, S. N. Stamenković, B. Č. Popović, *Europhys. Lett.* **2012**, *100*(4), 45002.
[11] D. Dorozhkina, V. Semenov, T. Olsson, D. Anderson, U. Jordan, J. Puech, L. Lapierre, M. Lisak, *Phys. Plasmas* **2006**, *13*(1), 013506.
[12] J. Foster, H. Krompholz, A. Neuber, *Phys. Plasmas* **2011**, *18*(1), 013502.
[13] A. P. Jovanović, B. Č. Popović, V. Lj. Marković, S. N. Stamenković, M. N. Stankov, *Eur. Phys. J. Appl. Phys.* **2014**, *67*(2), 20801.
[14] Z. Donkó, *Phys. Rev. E* **1995**, *51*, 3934.
[15] M. Puač, D. Marić, M. Radmilović-Radjenović, M. Šuvakov, Z. Lj. Petrović, *Plasma Sources Sci. Technol.* **2018**, *27*(7), 075013.
[16] J. Chew, P. Gibbon, D. Brömmel, T. Wauters, Y. Gribov, P. de Vries, *Plasma Phys. Control. Fusion* **2021**, *63*(4), 045012.
[17] A. Settaouti, *Electr. Eng.* **2010**, *92*(1), 35.
[18] B. J. P. Dowds, R. K. Barrett, D. A. Diver, *Phys. Rev. E* **2003**, *68*(2), 026412.

[19] S. Mirpour, A. Martinez, J. Teunissen, U. Ebert, S. Nijdam, *Plasma Sources Sci. Technol.* **2020**, *29*(11), 115010.
[20] A. M. Lietz, E. V. Barnat, G. R. Nail, N. A. Roberds, A. S. Fierro, B. T. Yee, C. H. Moore, P. G. Clem, M. M. Hopkins, *J. Phys. D: Appl. Phys.* **2021**, *54*(33), 334005.
[21] I. V. Schweigert, M. M. Hopkins, E. Barnat, M. Keidar, *Plasma Sources Sci. Technol.* **2022**, *31*(3), 03LT01.
[22] F. Ghaleb, A. Belasri, *Radiat. Eff. Defects Solids* **2012**, *167*(6), 377.
[23] A. P. Jovanović, M. N. Stankov, V. Lj. Marković, S. N. Stamenković, *Europhys. Lett.* **2013**, *104*(6), 65001.
[24] M. N. Stankov, M. D. Petković, V. Lj. Marković, S. N. Stamenković, A. P. Jovanović, *Chinese Phys. Lett.* **2015**, *32*(2), 025101.
[25] B. Saleh, Photoelectron Statistics, Springer Series in Optical Sciences, Springer-Verlag, Berlin **1978**.
[26] A. P. Jovanović, S. N. Stamenković, M. N. Stankov, V. Lj. Marković, *Contrib. Plasma Phys.* **2019**, *59*(3), 272.
[27] H. R. Skullerud, *J. Phys. D: Appl. Phys.* **1968**, *1*(11), 1567.
[28] C. Costin, *Sci. Rep.* **2021**, *11*(1), 1874.
[29] S. F. Biagi, Biagi database, www.lxcat.net/Biagi-v7.1, retrieved on April 25, 2018.
[30] A. V. Phelps, Phelps database, www.lxcat.net/Phelps, retrieved on April 25, 2018.
[31] D. L. Scharfetter, H. K. Gummel, *IEEE Trans. Electron Devices* **1969**, *16*(1), 64.
[32] M. N. Stankov, M. D. Petković, V. Lj. Marković, S. N. Stamenković, A. P. Jovanović, *Rom. Journ. Phys.* **2014**, *59*(3–4), 328.
[33] M. N. Stankov, Ph.D. thesis, Faculty of Sciences and Mathematics, University of Niš, Višegradska 33, Niš, Serbia, **2015**.
[34] R. A. Wijsman, *Phys. Rev.* **1949**, *75*(5), 833.
[35] A. V. Phelps, Z. Lj. Petrović, *Plasma Sources Sci. Technol.* **1999**, *8*(3), R21.
[36] V. Lj. Marković, Z. Lj. Petrović, M. M. Pejović, *J. Chem. Phys.* **1994**, *100*(11), 8514.

How to cite this article: A. P. Jovanović, M. N. Stankov, V. Lj. Marković, S. N. Stamenković, *Contrib. Plasma Phys*. **2023**, *63*(3-4), e202200161. https://doi.org/10.1002/ctpp.202200161